ISSN:3007-9640 DOI: https://doi.org/10.70114/acmsr.2025.2.1.P152

Excavation Effects on Deep and Large Circular working well

Yiming Liu [1]

[1] Shenzhen Research and Design Institute of China Academy of Railway Sciences, 518054, Shenzhen;

[a] 1013719403@qq.com

Abstract: This paper investigates the excavation effects on deep and large circular working well, focusing on the Shenzhen-Da intercity railway project between Pingshan Station and Julong Station in Shenzhen. The study examines the computational models and the force and deformation characteristics of circular working shaft support structures. The engineering challenges include complex geological conditions with significant soil layer variations. The circular support structure effectively converts water and soil pressure into circumferential pressure, leveraging the compressive strength of concrete to provide stability and rigidity. The research utilizes both field measurements and numerical simulations to analyze the deformation and stability of the retaining walls. Key findings include the effectiveness of circular underground continuous walls in providing self-stability and the impact of geological undulations on wall deformation. The study also highlights the importance of the ratio of shaft diameter to depth in maintaining structural stability. The results offer valuable insights for similar projects, emphasizing the need for careful design considerations to ensure safety and cost-effectiveness.

Keywords: Working well; Circular foundation pit; Size effect; Numerical analysis

1. Introduction

In recent years, with the increasing number of intercity railway tunnel sections in Shenzhen, many super deep working shaft excavation pits with depths exceeding 35 meters have emerged. The strata are mostly bimodal soil-rock formations with complex geological conditions and significant soil layer variations, which increase the difficulty of design and construction. Circular working shaft support structures can transform the water and soil pressure acting on the retaining walls into circumferential pressure on the circular support structure, fully utilizing the compressive strength of concrete. They possess good self-stability, strong overall rigidity, and small radial deformation, making them an economical and rational type of underground space structure [1-5]. This paper, based on the super deep circular working shaft project of the Shenzhen section of the Shenzhen-Da intercity railway from Pingshan Station to Julong Station, studies the calculation model of circular working well and the force and deformation characteristics of their support structures. The project has certain reference significance and practical value for saving project costs, shortening construction periods, and subsequent similar projects.

2. Project Introduction

2.1 Project Overview

The Shenzhen International Airport-Dayawan Intercity Railway is located in the northern part of Shenzhen City, with an overall east-west orientation. The line starts from the T4 hub of Bao'an Airport in Shenzhen and ends at Julong Station. The Pingshan-Julong interval working shaft is constructed using the open cut method, with an inner diameter of 36 meters and a depth of about 44 meters. The upper part of the excavation pit uses an 800mm thick circular cantilever underground continuous wall + 6 ring frame beams + 1 prestressed anchor support method, where the thickness of the underground continuous wall is 0.8 meters, with the bottom of the wall embedded in the moderately weathered layer by no less than 2.5 meters, or in the slightly weathered layer by no less than 1.5 meters; the lower part of the excavation pit uses an anchor spray support method. The plan

ISSN:3007-9640 DOI: https://doi.org/10.70114/acmsr.2025.2.1.P152

view of the excavation pit and the cross-section of the retaining structure are shown in Figures 1 and 2, respectively.

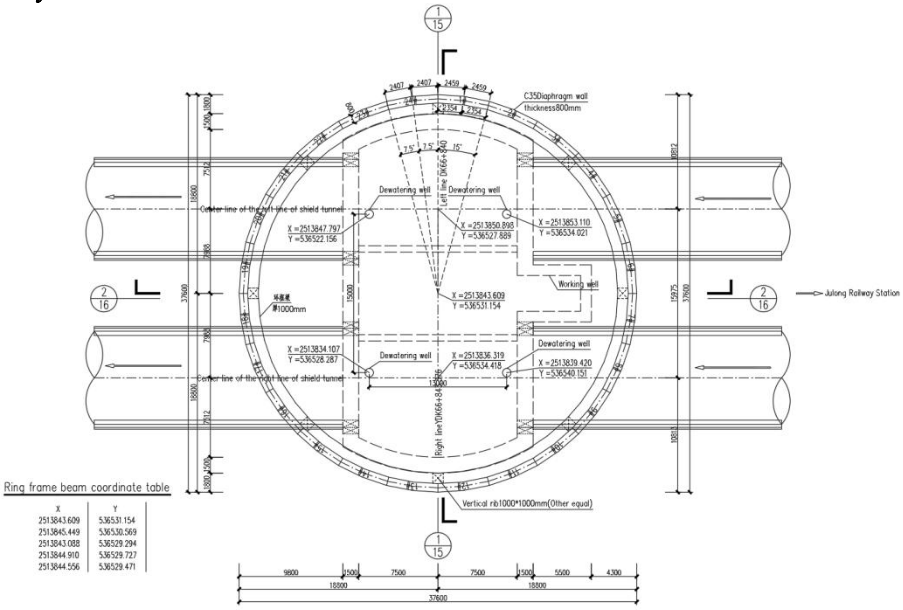

Fig. 1 Working well envelope structure plan

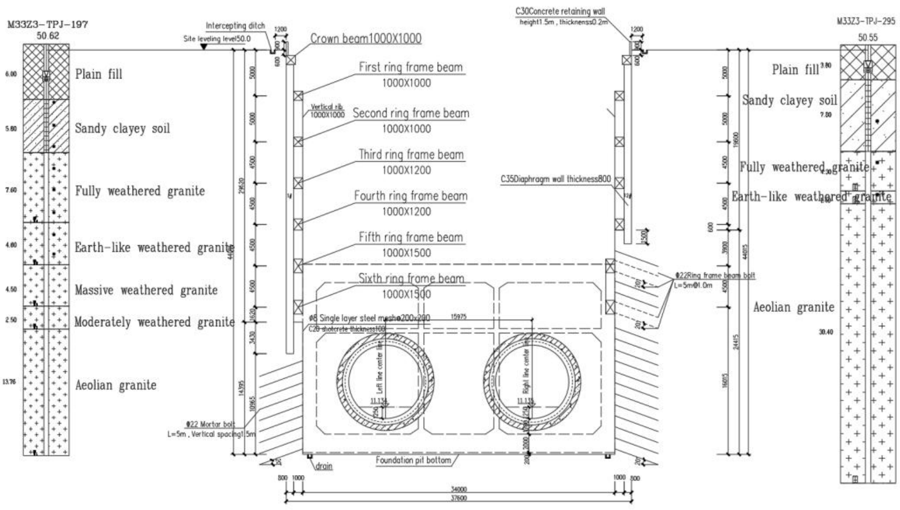

Fig. 2 Pit 1-1 profile

2.2 Engineering Geology and Hydrogeology

The main strata exposed in the Pingshan-Julong interval site are the Quaternary Holocene artificial fill layer, the Quaternary Holocene alluvial and fluvial layer, the Quaternary residual layer, and the Yanshanian fourth and second phase granite. The soil layers of the working shaft excavation pit from top to bottom are: plain fill soil, sandy clay, fully weathered granite, soil-like strongly weathered granite, blocky strongly weathered granite, moderately weathered granite, and slightly weathered granite. The physical and mechanical properties of each soil layer are shown in Figure 3, and the engineering geological distribution is shown in Figure 4.

The surface water in the site area is mainly from Tangwai Kou Reservoir and ponds. The main source of replenishment for the pore water of the loose rock class is atmospheric precipitation, and the replenishment amount is affected by the atmospheric rainfall and the infiltration coefficient. The main discharge methods are underground runoff and evaporation discharge. There is no stable aquiclude between the pore water and the bedrock fracture water, and there is a certain hydraulic connection between the two layers of groundwater. During this survey, the groundwater level was measured to be buried at a depth of 1 to 9.9 meters. According to the experience in Shenzhen area,

ISSN:3007-9640 DOI: https://doi.org/10.70114/acmsr.2025.2.1.P152

the groundwater level change amplitude in the plain area is 0.5 to 2 meters, and in the hilly and tableland areas, it is about 2 to 5 meters.

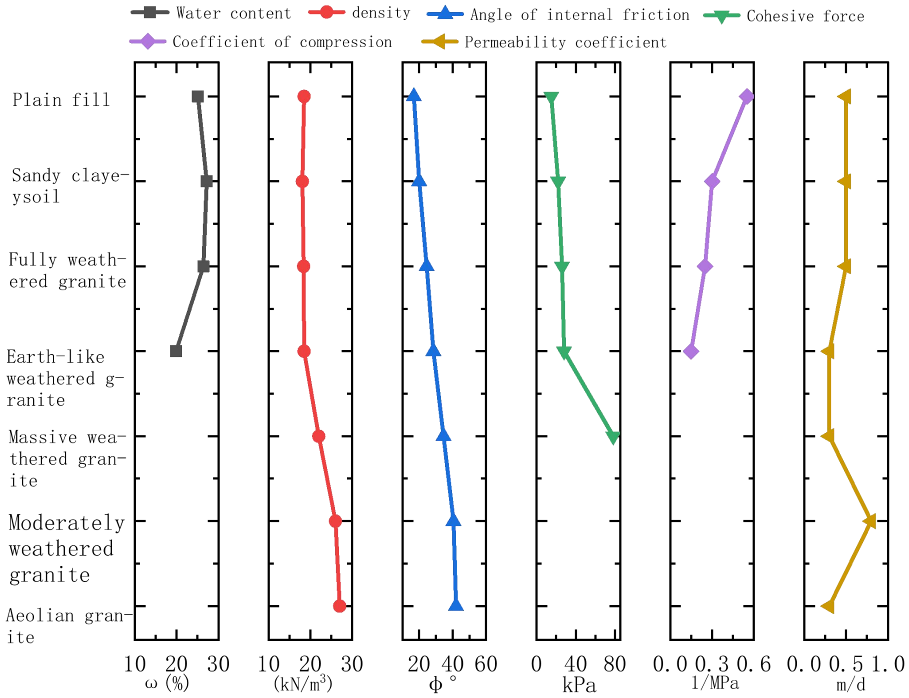

Fig. 3 Soil layer physical and mechanical parameters

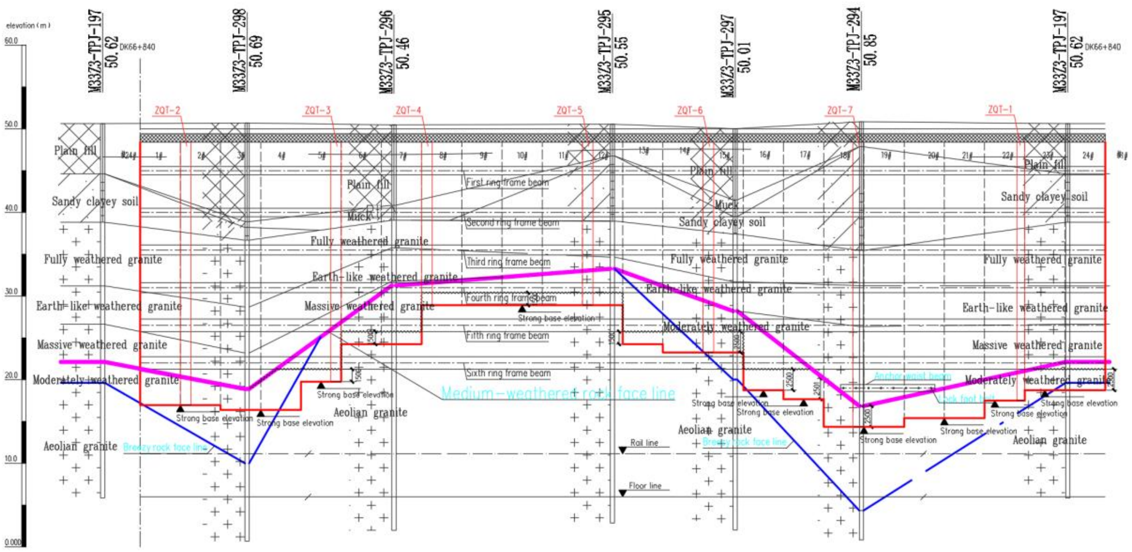

Fig. 4 Engineering geological distribution map

2.3 Monitoring Plan

A set of deep horizontal displacement monitoring holes for the underground continuous wall is arranged every 14 meters around the working shaft, with a total of 7 sets. The layout position of the monitoring points and the geological conditions of the monitoring points are shown in Figure 4. A set of horizontal displacement and vertical settlement monitoring points for the top of the underground continuous wall is arranged every 14 meters around the working shaft, with a total of 6 sets. Four to five ground settlement monitoring sections are arranged within twice the excavation depth of the excavation pit in the vertical direction of the excavation pit, with a total of 55 settlement monitoring points. At the same time, the settlement of underground pipelines and surrounding buildings within the excavation influence range is monitored. The layout of the monitoring points is shown in Figure 5.

ISSN:3007-9640 DOI: https://doi.org/10.70114/acmsr.2025.2.1.P152

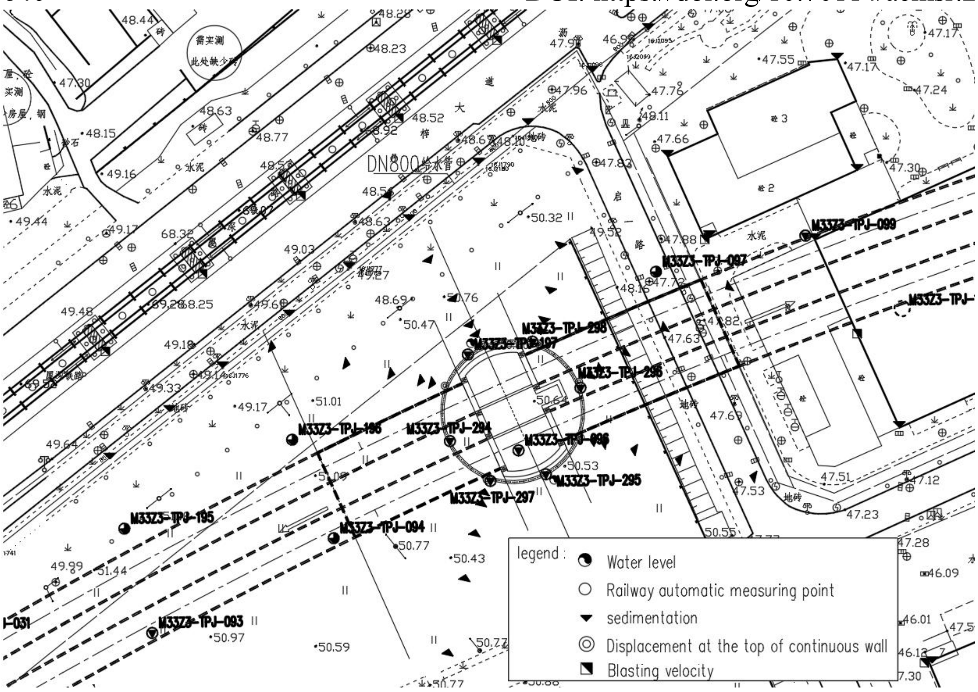

Fig. 5 Monitoring site layout plan

3. Analysis of Monitoring Data

Figure 6 shows the change curve of the horizontal displacement of the underground continuous wall after excavation to the bottom of the pit. Overall, the higher the bedrock surface, the smaller the horizontal displacement of the continuous wall: the bedrock surface depth of monitoring point ZQT-1 is -29 meters, and the corresponding maximum horizontal displacement of the continuous wall is 8.4 mm; the bedrock surface depth of monitoring point ZQT-5 is -15 meters, and the corresponding maximum horizontal displacement of the continuous wall is 2.3 mm; the bedrock surface depth of monitoring point ZQT-6 is -19 meters, and the corresponding maximum horizontal displacement of the continuous wall is 6.4 mm. Among all monitoring points, the maximum horizontal displacement is 11.3 mm, which is far less than the control value of 30 to 50 mm specified in the standard [6]. From Figure 4, it can be seen that monitoring point ZQT-4 is located at the center of the rock surface protrusion, with a rock surface depth of -15 meters, and the bedrock surface depths corresponding to monitoring points ZQT-1 and ZQT-7 are the deepest, with a rock surface depth of -29 meters. Under the action of soil pressure behind the wall, the excavation pit presents a significant eccentric pressure characteristic. The circular continuous wall is mainly subjected to circumferential compression, and under the eccentric pressure load, the section at ZQT-4 is subjected to obvious compression, causing the wall to move outward as a whole. The upper soil has a slightly poorer ability to resist deformation, while the lower bedrock has a stronger ability to resist deformation, so the horizontal displacement curve of the continuous wall shows an "overhanging" distribution with a larger upper part and a smaller lower part.

The bottom of the excavation pit is all below the bedrock surface, and the continuous wall forms a "cantilever" structure. The design depth of the continuous wall in this project is to embed into the moderately weathered rock by no less than 2.5 meters. The distance between the bottom of the shallowest continuous wall and the bottom of the pit is 23 meters. In this case, the displacement of the bottom of the continuous wall at each monitoring point is basically 0, and the prestressed anchor can effectively limit the displacement of the bottom of the wall. The design of the retaining structure of this project is reasonable, and the overall deformation of the continuous wall is significantly smaller than that of the traditional rectangular underground continuous wall. The circular underground continuous wall has a good three-dimensional spatial arch effect. The support method of cantilever underground continuous wall + 6 ring frame beams fully utilizes the

ISSN:3007-9640 DOI: https://doi.org/10.70114/acmsr.2025.2.1.P152

self-stability performance of the circular excavation pit, effectively ensuring the safety and stability of the excavation pit during the excavation process.

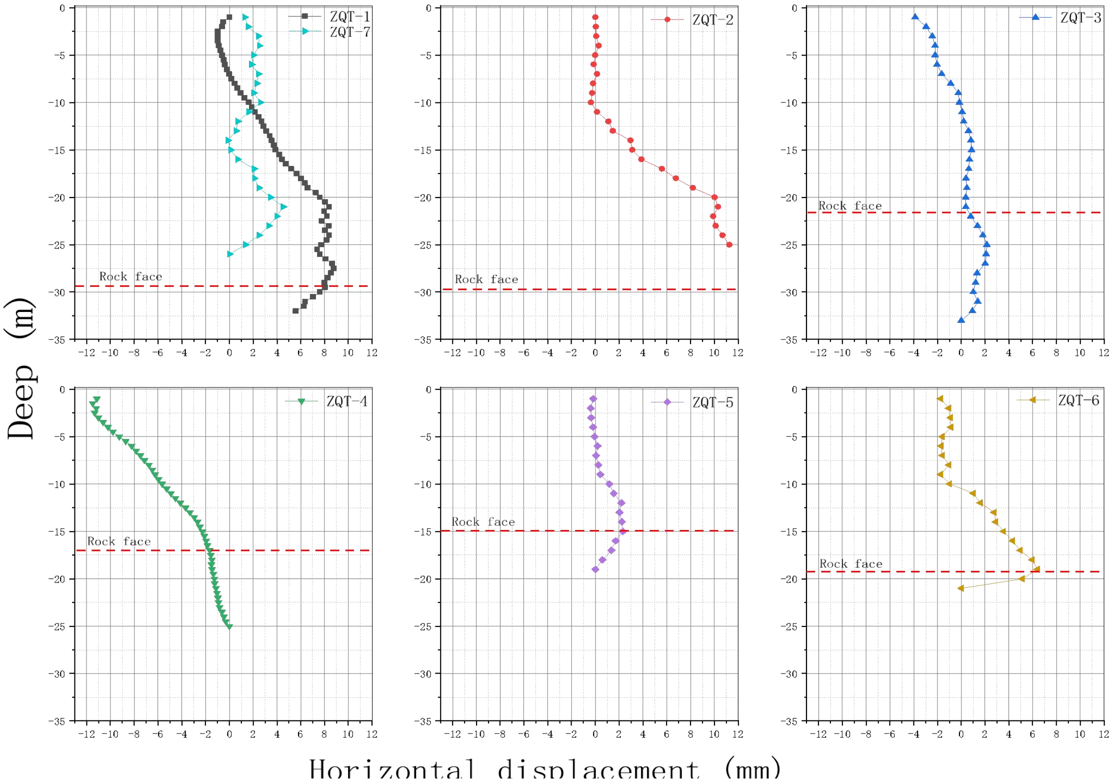

Fig. 6 Horizontal displacement curve of underground diaphragm wall after excavation

Figure 7 shows the schematic diagram of the change in the horizontal displacement of the top of the continuous wall after the excavation pit is excavated to the bottom, representing the change in the shape of the wall top before and after deformation. From the figure, it can be seen that due to the lack of internal support in the excavation pit, the overall stiffness of the wall top is insufficient under the influence of soil pressure behind the wall, resulting in a certain deformation. At the same time, due to the eccentric pressure effect formed by the geological undulations, the continuous wall is compressed towards the shallow rock surface. Among them, ZQS-06 moves outward by 12.6 mm, and ZQS-04 moves outward by 5.4 mm. After deformation, the continuous wall finally presents a "teardrop-shaped" deformation pattern.

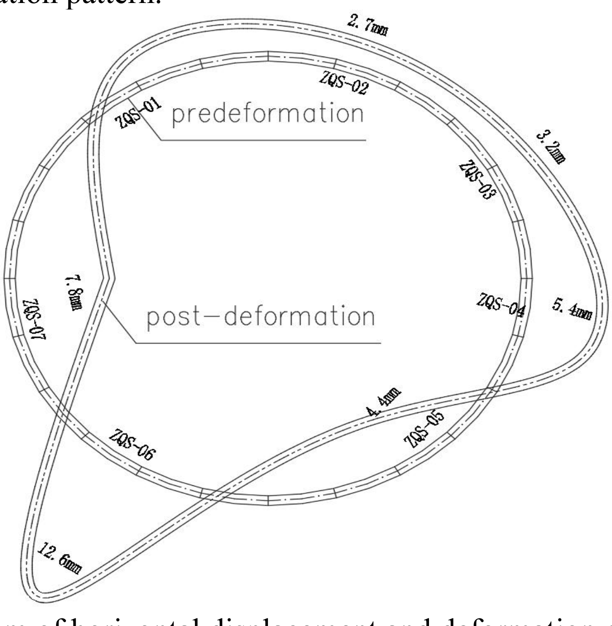

Fig. 7 Comparison diagram of horizontal displacement and deformation on top of continuous wall

ISSN:3007-9640 DOI: https://doi.org/10.70114/acmsr.2025.2.1.P152

4. Numerical Analysis

4.1 Establishment of Numerical Model

According to the standard [7], when the circular underground continuous wall support structure uses the inner ring beam as support, the inner ring beam can be replaced with an equivalent elastic support. The equivalent elastic coefficients per unit width of the wall are calculated as shown in Table 1.

Table 1. Table of equivalent elastic coefficients

specification	Equivalent elastic coefficients（kN/m）	remark
1.0m×1.0m Crown beam	89582	C30
1.0m×1.0m Ring beam	97959	C30
1.0m×1.2m Ring beam	117551	C30
1.0m×1.5m Ring beam	146938.8	C30
0.8m Diaphragm wall	29015	C35

Taking the most unfavorable geological condition of borehole M33Z3-TPJ-294, the soil layers within the working shaft range from top to bottom are 2.15 meters thick plain fill soil, 12.40 meters thick sandy clay, 4.20 meters thick fully weathered granite, 4.90 meters thick soil-like strongly weathered granite, 9.50 meters thick blocky strongly weathered granite, and 12.50 meters thick moderately weathered granite. A two-dimensional calculation model is established as shown in Figure 8, and the calculation and analysis are carried out using the Lizheng Deep Excavation software.

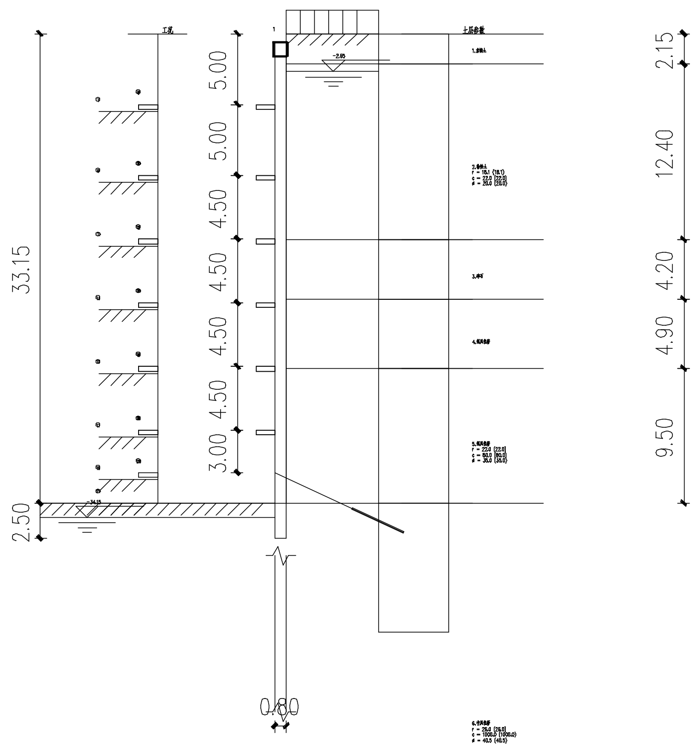

Fig. 8 Two-dimensional computational model diagram

A three-dimensional spatial structural model of the force on the circular working shaft retaining structure is established using the Midas GTS software to analyze the mechanical response of the circular working shaft retaining structure. To reduce the impact of errors, the following basic assumptions are made in this paper: each layer of rock and soil is a homogeneous and isotropic material; the rock and soil are ideal elastoplastic materials; the retaining structure is a linear elastic material; the seepage effect of groundwater is not considered. The model has an inner diameter of

ISSN:3007-9640 DOI: https://doi.org/10.70114/acmsr.2025.2.1.P152

36 meters, an excavation depth of 44 meters, an underground continuous wall thickness of 0.8 meters, and an embedded depth of 2.5 meters. The planar dimensions of the model are twice the excavation depth of the pit, with the overall model dimensions being 100m × 100m × 70m (length, width, height). The three-dimensional model of the working shaft is shown in Figure 9. The Mohr-Coulomb constitutive model is used for calculation, and the physical and mechanical parameters of each stratum are shown in Table 2.

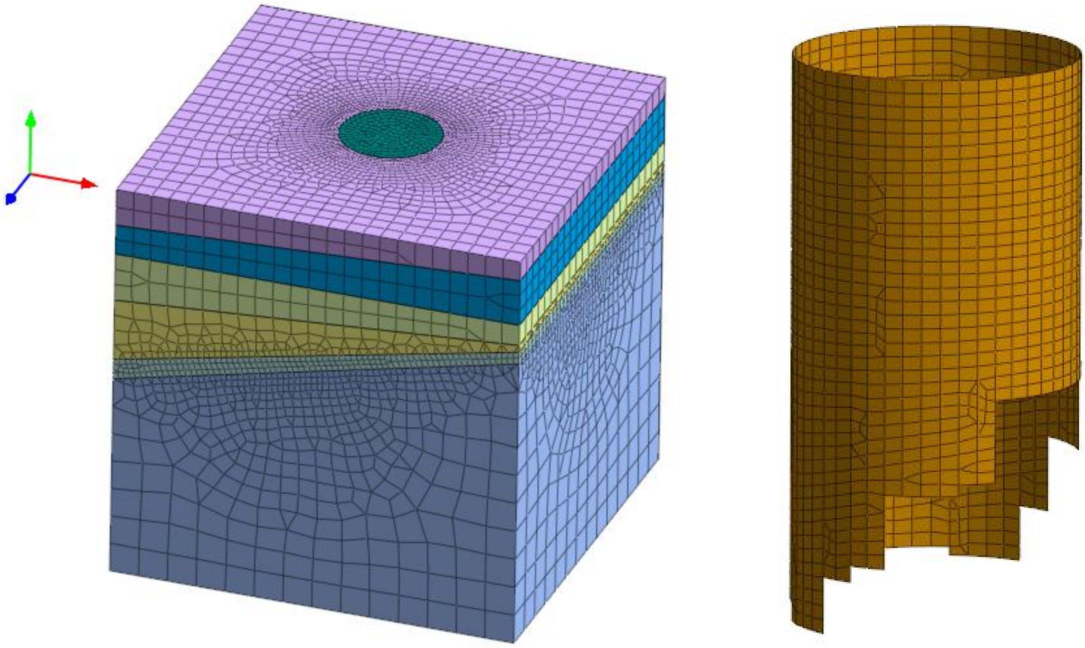

Fig. 9 3D model diagram of working well

Table 2. Physical and mechanical index design parameter table

Soil layer	Density (kg/m3)	Cohesive force (kPa)	Angle of internal friction (°)	Modulus of elasticity (kPa)
Plain fill	1.83	8	5	4000
Sandy clayeysoil	1.77	23	18.5	35000
Fully-weathered-granite	1.8	30	25	50000
Earth-like-weathered-granite	1.85	28	35	100000
Massive-weathered-granite	2.2	80	40	150000
Moderately-weathered-granite	2.7	/	42	2.50E+06
Aeolian granite	2.7	/	45	5.00E+06

4.2 Comparison of Calculation Results

Figure 10 shows the comparison between the numerical simulation calculation results and the measured values of the horizontal displacement at the top of the wall. From the figure, it can be seen that the horizontal displacement at the top of the wall increases with the increase of excavation depth. The maximum measured horizontal displacement at the top of the wall is about 12.6 mm, and the maximum finite element calculated horizontal displacement at the top of the wall is about 8.6 mm. The simulation results are basically consistent with the measured results, and the numerical simulation parameters are reasonably selected, ensuring the accuracy of subsequent analysis.

ISSN:3007-9640 DOI: https://doi.org/10.70114/acmsr.2025.2.1.P152

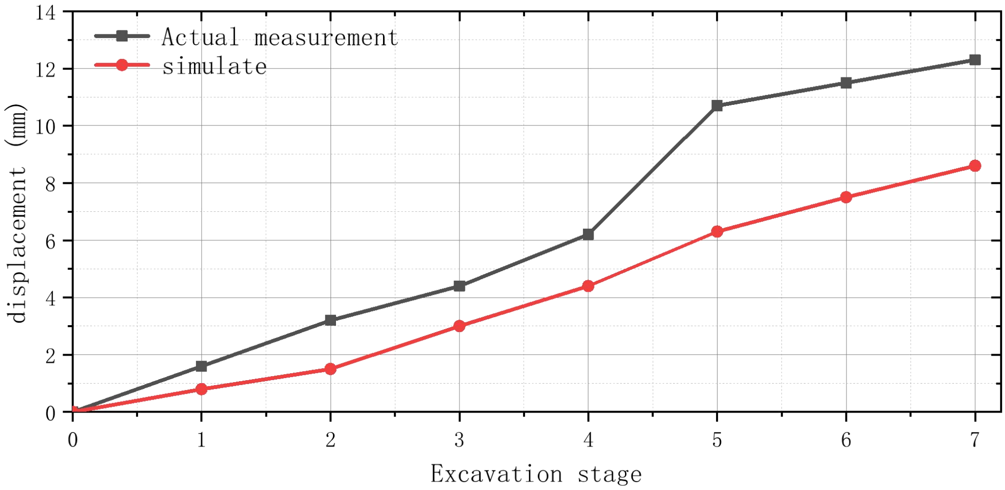

Fig. 10 Comparison between numerical simulation and measured results of Horizontal displacement of the top of the wall

At the same location of the working shaft, the wall displacement obtained from the two-dimensional elastic support model and the three-dimensional stratum structure model is compared with the measured results, as shown in Figure 11. From the figure, it can be seen that the three-dimensional simulation calculation and the measured results are close, both showing an "overhanging" distribution, with the maximum horizontal displacement of the wall being less than 12 mm. However, the two-dimensional calculation shows an "inward convex" distribution of the wall horizontal displacement, and the maximum displacement is greater than 24 mm, which is significantly larger than the three-dimensional simulation and measured results. Observing the three-dimensional calculation result cloud map, it can be seen that under the action of eccentric pressure, the excavation pit shows a typical compression effect, with the shallower rock surface being compressed outward as a whole, and the continuous wall shows a "teardrop-shaped" deformation pattern, which is consistent with the measured results.

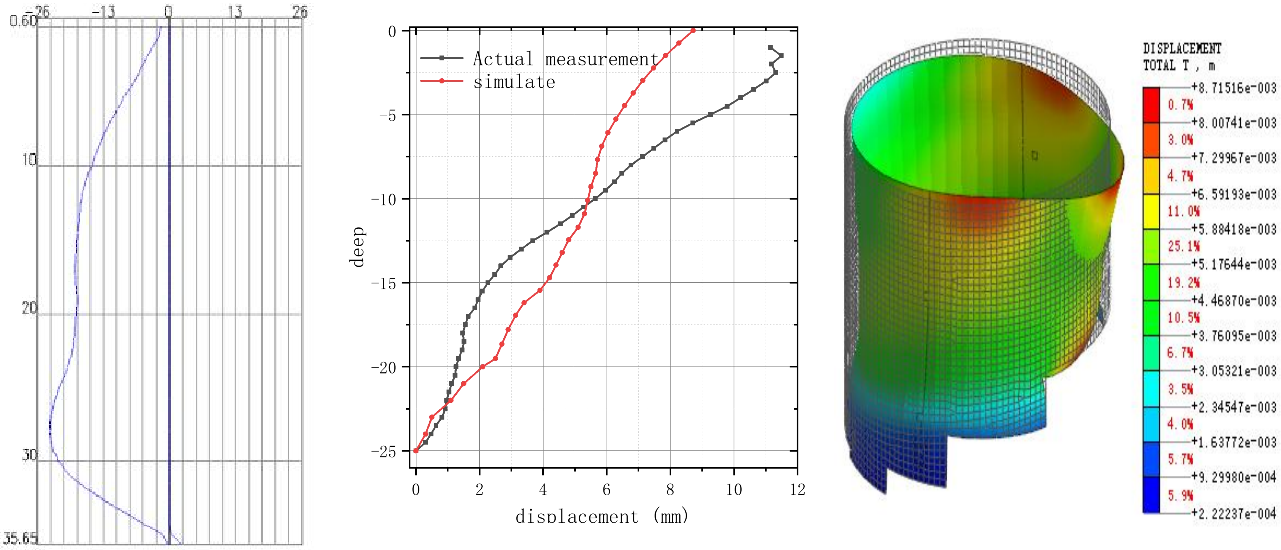

a Two-dimensional result

b Three-dimensional calculation results and measured results

c 3D computed cloud image

Fig. 11 Comparison of calculation results of wall horizontal displacement

The distribution of the vertical bending moment (moment vector direction along the vertical direction of the underground continuous wall) and the horizontal bending moment (moment vector direction along the circumferential direction of the underground continuous wall) of the

ISSN:3007-9640 DOI: https://doi.org/10.70114/acmsr.2025.2.1.P152

underground continuous wall is shown in Figure 12. From the figure, it can be seen that since the underground continuous wall is a quasi-circular structure, it also generates a certain vertical bending moment under the action of water and soil pressure, causing it to exhibit a bending and compressive stress state in the circumferential direction. The maximum value of the vertical bending moment is mainly distributed in the area of the underground continuous wall near the bottom of the excavation pit. The horizontal bending moment of the underground continuous wall is mainly caused by the lateral action of water and soil pressure, and the difference between the horizontal bending moment of the straight section of the underground continuous wall and the horizontal bending moment at the inflection point is not significant. At the same location, the wall bending moment and shear force calculated by the two-dimensional method are 1240.5 kN·m and 773.2 kN, respectively, while the wall bending moment and shear force calculated by the three-dimensional method are 130.0 kN·m and 430.0 kN, respectively. Combining the deformation characteristics of the continuous wall, it can be seen that when using the two-dimensional elastic support model for calculation, although the circumferential support effect of the circular underground continuous wall is considered through the equivalent support spring, the calculation results of force and deformation are still larger than those of the three-dimensional calculation, and the calculation results are more conservative.

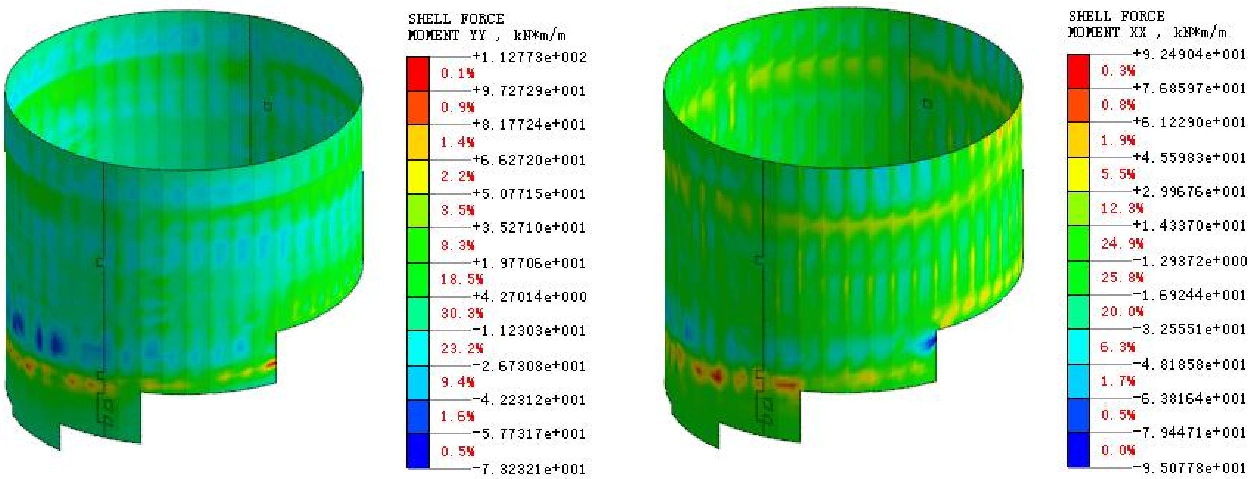

a Vertical bending moment b Transverse bending moment

Fig. 12 3D computed moment distribution cloud image

4.3 Analysis of the Influence of Working Shaft Dimensions

The ratio of diameter D to depth L is used as the influencing parameter for calculation and analysis. The calculation cloud map of wall displacement is shown in Figure 13. From the figure, it can be seen that under a certain depth, as the diameter of the excavation pit increases, the horizontal displacement of the continuous wall continues to increase, and the resistance to deformation of the upper part of the continuous wall gradually decreases. The difference in wall deformation is mainly reflected in the upper part of the excavation pit, and the deformation of the lower part of the excavation pit is strongly limited due to the embedding in the moderately weathered rock layer. The curve of the maximum horizontal displacement of the wall with the change of the excavation pit diameter D is shown in Figure 14. It can be seen that within the diameter range of 0.5L to 2L, the deformation of the continuous wall increases slowly, and when the diameter exceeds 2L, the deformation of the continuous wall increases rapidly, indicating that the support form of the inner frame beam no longer meets the stability requirements of the excavation pit. Therefore, in the design of similar excavation pit projects, the ratio of the excavation pit diameter D to the depth L should be controlled within 2.

ISSN:3007-9640 DOI: https://doi.org/10.70114/acmsr.2025.2.1.P152

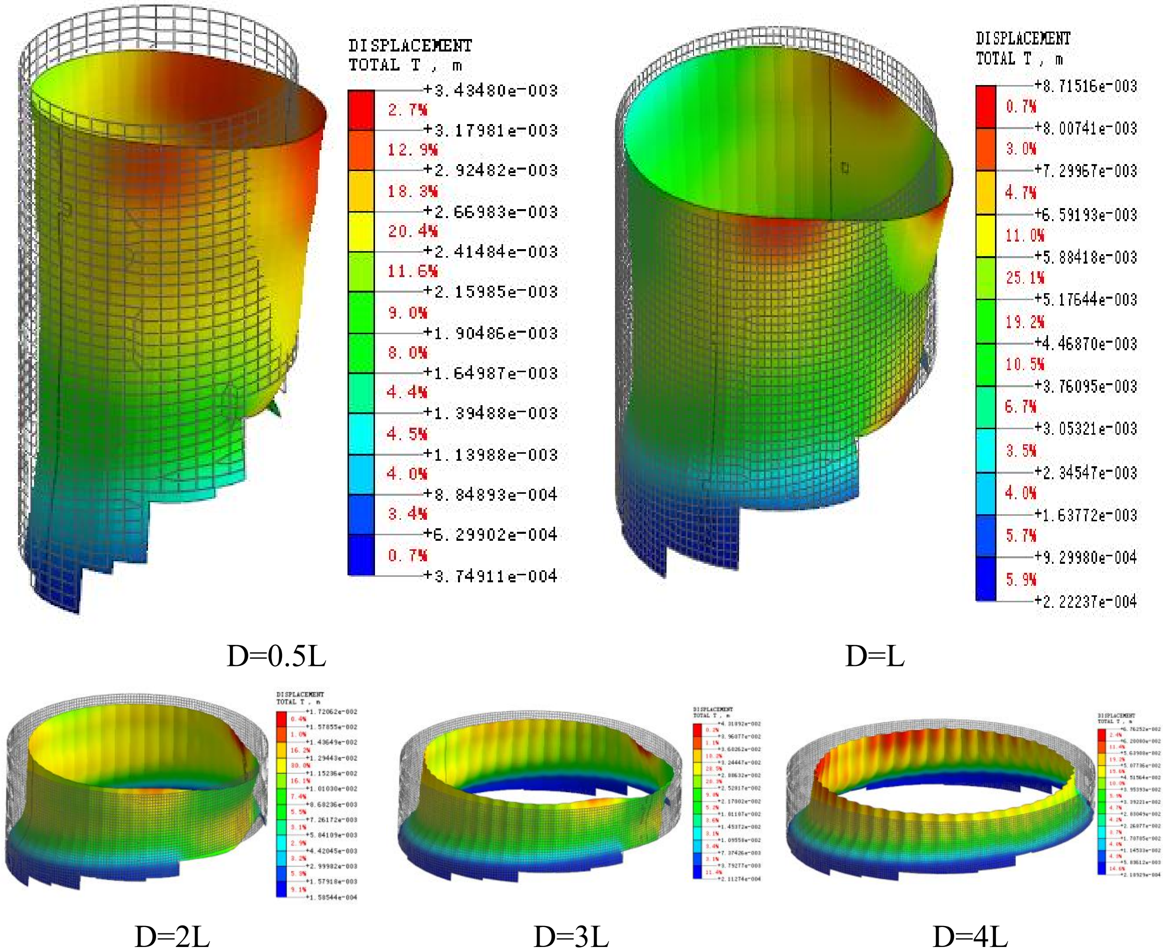

Fig. 13 Cloud image of horizontal displacement calculation results of continuous wall under different diameters of foundation pit

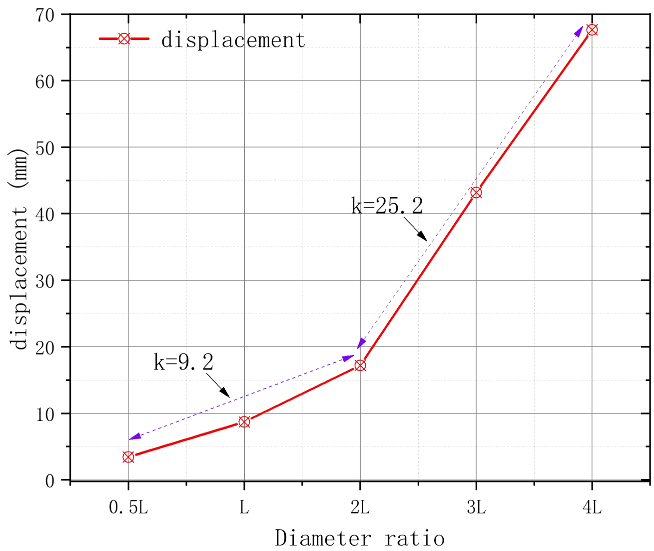

Fig. 14 The change of maximum horizontal displacement with the diameter of foundation pit

5. Conclusion

Based on the example of the working shaft excavation pit project in the Pingshan-Julong interval, this paper uses the methods of measured analysis and numerical simulation to systematically

ISSN:3007-9640 DOI: https://doi.org/10.70114/acmsr.2025.2.1.P152

analyze the deformation and force characteristics of the circular excavation pit, and the following conclusions are drawn:

(1) The circular underground continuous wall has a good three-dimensional spatial arch effect. The support method of cantilever underground continuous wall + 6 ring frame beams fully utilizes the self-stability performance of the circular excavation pit, effectively ensuring the safety and stability during the excavation process.

(2) The geological undulations form an eccentric pressure effect. Since the excavation pit is not equipped with internal support, the continuous wall is compressed towards the shallow rock surface, and the continuous wall finally presents a "teardrop-shaped" deformation pattern. In future similar projects, the first support can be considered to further ensure the safety and stability of the excavation pit.

(3) When using the two-dimensional elastic support model for calculation, although the circumferential support effect of the circular underground continuous wall is considered through the equivalent support spring, the calculation results of force and deformation are still larger than those of the three-dimensional calculation, and the calculation results are more conservative. This method can be used for calculation in design.

(4) As the diameter of the excavation pit increases, the horizontal displacement of the continuous wall continues to increase. When the diameter exceeds 2L, the deformation of the continuous wall increases rapidly. In the design of similar excavation pit projects, the ratio of the excavation pit diameter D to the depth L should be controlled within 2.

Acknowledgment

This research was funded by Funds of China Academy of Railway Sciences Group Co., Ltd. (No. 2023YJ243).

References

[1] Zhao Yixing, Zhan Gangyi, Shi Yufeng, et al. Effect and optimization of the inner lining wall of the ultra-deep circular foundation pit in the soil-rock composite stratum[J]. Journal of Jilin University (Earth Science Edition), 2023, 53(2): 526-540.

[2] Zong Ludan, WANG Weidong, XU Zhonghua, et al. Mechanical properties of a 56 m deep circular shaft foundation pit support structure in soft soils[J]. Tunnel construction, 2022, 42(7): 1248-1256.

[3] Zhai Jiequn, XIE Xiaolin, JIA Jian. Design method for large-deep circular foundation pit of Shanghai Tower[J]. Chinese journal of geotechnical engineering, 2010, 32(S1): 392-396.

[4] Weng Qiping, WANG Weidong, ZHOU Jianlong. Design of diaphragm of an ultra-deep cylindrical excavation constructed by top-down method [J]. Journal of Building Structure, 2010, 31(5): 192.

[5] Han Weijie, Yang Guofu, Cao Chengyong, et al. Size Effect of Deep Circular Working Shaft Excavation for Rail Transit Construction[J]. Urban Rapid Rail Transit, 2024, 37(06): 99-105.

[6] GB 50497-2019 Technical Standard for Monitoring of Building excavation Engineering.

[7] JTG 3363-2019 Specifications for Design of Foundation of Highway Bridges and Culverts.